

Physics of Transcendental Numbers Meets Gravitation

Hartmut Müller

E-mail: hm@interscalar.com

Transcendental ratios of physical quantities can provide stability in complex dynamic systems because they inhibit the occurrence of destabilizing resonance. This approach leads to a fractal scalar field that affects any type of physical interaction and allows reformulating and resolving some unsolved tasks in celestial mechanics and astrophysics. We verify the model claims on the gravitational constants and the periods of orbital and rotational motion of the planets, planetoids and large moons of the solar system as well as the orbital periods of exoplanets and the gravitational constants of their stars.

Introduction

Despite the abundance of theoretical approaches engaged to explain the origin of gravitational interaction dealing with superstrings, chameleons or entropic forces [1], the community of physicists still expects compatibility for centuries: any modern theory must allow deriving Newton's law of universal gravitation as classic approximation. In the normal case of weak gravity and low velocities, also Einstein's field equations obey the correspondence principle.

Besides of nostalgia, what could be the reason of this condition? Newton's law of gravitation cannot be verified in the scale of the solar system, because the mass of a planet cannot be measured, and Kepler's laws of planetary motion do not compellingly require Newton's law of gravitation for their derivation. Moreover, Newton's theory of gravitation leads to inconsistencies already in the case of three interacting bodies.

It is a common belief that John Couch Adams and Urbain Le Verrier applying Newton's law of gravitation could predict the orbit and correct position of Neptune based on motions of Uranus. However, this is not exactly what they did.

Adopting the Titius-Bode law [2], Adams assumed the semi-major axis of Neptune being 37.25 AU; Le Verrier estimated 36.15 AU. The deviation from the correct value 30.07 AU is more than 20%. Adopting Pontécoulant's *Théorie Analytique* to his perturbation approach, Adams calculated an eccentricity of 0.1206; Le Verrier got 0.1076. The right value is 0.0086, a deviation of more than 1100%. Adams calculated the longitude of the perihelion being at 299°; Le Verrier arrived at 284° while the correct is 44°. Finally, applying Newton's law of gravitation, Adams estimated Neptune's mass with 1/6666 solar mass; Le Verrier calculated 1/9300. Actually, the ratio is 1/19300. Again, a deviation of > 200%. It is a miracle how with all these errors Le Verrier could guess the right longitude 326° of the current position of Neptune. Obviously, he was very lucky [3].

Kepler's laws of planetary motion cannot explain why the solar system has established the orbital periods 90560 days (Pluto), 60182 (Neptune), 30689 (Uranus), 10759 (Saturn), 4333 (Jupiter), 1682 (Ceres), 687 (Mars), 365 (Earth), 225 (Venus) and 88 days (Mercury), because there are infinitely

many pairs of orbital periods and distances that fulfill Kepler's laws. Einstein's field equations do not reduce the theoretical variety of possible orbits, but increases it even more.

But now, after the discovery of thousands of exoplanetary systems, we can recognize that the current distribution of the planetary and lunar orbits in our solar system is not accidental. Many planets in the extrasolar systems like Trappist 1 or Kepler 20 have nearly the same orbital periods as the large moons of Jupiter, Saturn, Uranus and Neptune [4]. That's amazing, because Trappist 1 is 40 light years away from our solar system and Kepler 20 nearly 1000 light years [5, 6].

The question is, why they prefer similar orbital periods if there are infinite possibilities? Obviously, there are orbital periods preferred anywhere in the galaxy. Why these orbital periods are preferred? What makes them attractive?

Despite perturbation models and parametric optimization, the reality of planetary systems is still a theoretical problem. The notoriously high failure rate of interplanetary missions, flyby anomalies [7] and unexpected accelerations of spacecraft indicate a profound lack of understanding gravity.

In spiral galaxies, the orbiting of stars around their centers seems to strongly disobey both Newton's law of universal gravitation and general relativity. Recently, an 85% dark matter universe is required for saving the conventional paradigm.

Perhaps the concept of gravitation itself requires a revision. Obviously, it is not about details, but an important part of the hole is missing. For finding the missing part, let us go back to the roots of the idea of gravitation ...

The empirical universality of free fall led ancient philosophers to the idea that weight could be a universal property of matter. For a long time, this observation underpinned the geocentric worldview powered by Aristoteles; he believed that heavier objects experience a higher gravitational acceleration.

Centuries later, in his famous book '*De revolutionibus orbium coelestium*', Nicolaus Copernicus (1543) interpreted weight as divine phenomenon by which all things, including stars, planets and moons, are brought toward one another. In the '*Astronomia nova*', Johannes Kepler (1609) compared weight with magnetism and hypothesized that any two stones attract each other in a way that is proportional to their masses. In the meantime, Galileo Galilei (1590) discovered that the

acceleration of free falling test bodies at a given location does not depend on their masses, physical state or chemical composition. Modern measurements [8] confirm Galilei's discovery with a precision of a trillionth. In a vacuum, indeed, a one gram light feather and a one kilogram heavy lead ball experience the same acceleration of free fall. Long time before Friedrich Bessel (1832) and Lorand Eötvös (1908), Galileo Galilei's discovery was experimentally confirmed by Isaak Newton (1680) comparing the periods of pendulums of different masses but identical length. Nevertheless, in his universal law of gravitation, Newton (1687) postulated that gravity depends on the masses of the involved bodies. Though, he was deeply uncomfortable with this idea. 26 years after the first publication of his "Principia", in the age of 71, Newton wrote: "I have not yet been able to discover the cause of these properties of gravity from phenomena and I feign no hypotheses." Newton recognized the importance of not confusing gravity acceleration with the force that gravity can cause [9]. Actually, the question is not, does the force caused by gravity depend on the masses of the moving bodies. The question is rather, does mass *cause* the acceleration of free fall.

Analyzing the astronomical observations of Tycho Brahe, Johannes Kepler (1619) discovered that for every planet, the ratio of the cube of the semi-major axis R of the orbit and the square of the orbital period T is constant for a given orbital system. In the case of the Earth, this ratio defines the geocentric gravitational constant μ . Kepler's discovery is confirmed by high accuracy radar and laser ranging of the motion of artificial satellites. Thanks to Kepler's discovery, Earth's surface gravity acceleration can be derived from the orbital elements of any satellite, also from Moon's orbit:

$$g = \frac{\mu}{r^2} = \frac{\mu}{(6378000 \text{ m})^2} = 9.81 \text{ m/s}^2,$$

$$\mu = 4\pi^2 \frac{R^3}{T^2} = 3.9860044 \cdot 10^{14} \text{ m}^3/\text{s}^2,$$

where R is the semi-major axis of Moon's orbit, T is the orbital period of the Moon and r is the equatorial radius of the Earth. No data about the masses or the chemical composition of the Earth or the Moon is needed.

Here it is important to underline that R and T are measured, but the identity $\mu = GM$ being the core of Newton's law of universal gravitation, is a theoretical presumption that provides mass as a source of gravity and the universality of the coefficient G as "gravitational constant".

One of the basic principles of scientific research is the falsifiability of a theory. Obviously, any theory that postulates gravitation of mass as forming factor of the solar system is not falsifiable, because there is no method to *measure* the mass of a planet. Actually, no mass of any planet, planetoid or moon is measured, but only calculated based on the theoretical presumption $\mu = GM$.

Naturally, G is estimated in laboratory scale where masses can be measured. However, not only the correctness of the

original experimental setup performed by Henry Cavendish (1798) is still under discussion, but also the correctness of more recent variants. There are large uncertainties not only in the obtained values of G , but even regarding the suitability of the applied methods of measuring gravity.

It is believed that gravitation cannot be screened. Because of this, it is virtually impossible to isolate the gravitational interaction between two masses from the presumed perturbative effects created by surrounding mass distributions. Invented by John Michell (1783), the instrument of choice for measuring G , the torsion pendulum, is subject to a variety of parasitic couplings and systematic effects which ultimately limit its suitability as a gravity transducer. George Gillies [10] listed about 350 papers almost all of which referred to work carried out with a torsion balance. Other sensitive mechanical devices are also pressed to the limits of their performance capabilities when employed for this purpose.

Besides of all the difficulties to measure G in laboratory, isn't there any other way to evidence the dependency of gravity on mass? For example, the Earth's surface masses are not uniformly distributed. There are huge mountains with a rock density of about three tons per cubic meter. There are oceans in which the density of water is only one ton per cubic meter - even at a depth of 10 kilometers. According to the logic of Newton's law of universal gravitation, these mass distribution inhomogeneities should act on sensitive gravimetric instruments. However, they do not [11].

In order to explain the absence of gravimetric evidence, the idea of isostasy [12] was invented. According to this hypothesis, the deeper the ocean, the more powerful the dense compensating deposits under its bottom; the higher the mountains, the looser is their foundation. Isostasy allegedly forms over huge periods of time, comparable to geological eras.

However, there are cases when very strong redistribution of surface masses occurs in a time period that is negligible by geological standards. For example, this happens during the eruption of an underwater volcano, when a seamount or even a new island builds up in a few days [13]. In these cases, there is no time to establish isostasy, and gravimetric instruments should react to these changes. Obviously, they do not react as expected, and for making gravity calculations more realistic, ground deformation data and numerical modelling is applied.

Gravimetric practice evidences that it is nearly impossible separating variations in gravity acceleration from low frequency seismic activity. Actually, gravimeters *are* long-period seismometers [14]. This is why the distribution of gravitational anomalies on gravity maps is indistinguishable from the zones of earthquakes and seismic activity.

Customarily, gravimetric data are recalculated with special corrections that providently consider the alleged effect of surface mass inhomogeneities. The corrections depend on the adopted model of the distribution of surface masses mainly based on seismic exploration. The idea to apply those corrections was proposed by Pierre Bouguer (1749). Now the dif-

ference between the really measured values of gravity and the theoretically calculated for an assumed mass density, is traditionally called a Bouguer-anomaly. Fluctuations in altitude of orbiting satellites indicating gravity variations are interpreted as caused by mass inhomogeneities [15]. In this way, gravimetric maps of planets and asteroids are being compiled.

In the case of mass as source of gravity, in accordance with Newton’s shell theorem, a solid body with a spherically symmetric mass distribution should attract particles outside it as if its total mass were concentrated at its center. In contrast, the attraction exerted on a particle should decrease as the particle goes deeper into the body and it should become zero at the body’s center.

The Preliminary Reference Earth Model [16] affirms the decrease of the gravity acceleration with the depth. However, this hypothesis is still under discussion. In 1981, Stacey, Tuck, Holding, Maher and Morris [17, 18] reported anomalous measures (larger values than expected) of the gravity acceleration in deep mines and boreholes. In [19] Frank Stacey writes that “geophysical measurements indicate a 1% difference between values at 10 cm and 1 km (depth); if confirmed, this observation will open up a new range of physics.”

Furthermore, measurements of G are notoriously unreliable, so the constant is in permanent flux and the official value is an average. If G is changing, then G could depend on a new field. But this could also evidence that gravity itself may be changing. As mentioned Terry Quinn [20] of the Bureau International des Poids et Mesures (BIPM), the discrepant results may demonstrate that we do not understand the metrology of measuring weak force or signify some new physics.

Introduced with the postulated equation $\mu = GM$ as coefficient compensating the dimension of mass, G has no known confirmed dependence on any other fundamental constant. Suppose G would be estimated to be two times larger than the currently recommended value, this would simply mean that the masses of celestial bodies would be estimated to be two times smaller. However, this change would not have any impact on calculations depending on μ . In this case, the hypothesis that mass *causes* gravity, could turn out to be a dispensable assumption.

In view of this situation, it is understandable to intensify the search of possible derivations of G from theory. As mentioned Gillies [10], some recent approaches seek the ad hoc introduction of a new field or effect to create a situation in which a value for G can be built from ratios of other fundamental constants and numerical factors. However, most of the attempts come from a general relativistic starting point to examine the outcome of some scenario in which G arises from the calculations. For instance, Yanpeng Li [21] derives

$$G = \frac{1}{16 \pi \cdot c \cdot \eta} = 6.636 \cdot 10^{-11} \text{ m}^3 \text{ kg}^{-1} \text{ s}^{-2}$$

from general relativity by introducing the “eigen-modulus of a tensor” as measure of its converging ability. According to

Li, the eigen-modulus of the Einstein tensor equals $1/16 \text{ m/s}^3$, the mass density $\eta = 1 \text{ kg/m}^3$ comes from the eigen-modulus of the energy-momentum tensor, c is the speed of light. Despite the numerical fit of the derived G value with the wide spectrum of data achieved in laboratory, the generality of this derivation and the physical sense of a mass density that equals 1 kg/m^3 may be questioned.

Introducing his geometric theory of gravitation, a century ago Einstein supposed that gravity is indistinguishable from, and in fact the same thing as, acceleration. Identifying gravity with acceleration $g = c \cdot f$, the gradient of a conservative gravitational field can be expressed in terms of frequency shifts:

$$\frac{\Delta f}{f} = g \frac{\Delta h}{c^2}.$$

Already in 1959, Robert Pound and Glen Rebka [22] verified this equation in their famous gravitational experiment. Sending gamma rays over a vertical distance of $\Delta h = 22.56 \text{ m}$, they measured a blueshift of $\Delta f/f = 2.46 \cdot 10^{-15}$ that corresponds precisely with Earth’s surface gravity 9.81 m/s^2 .

Actually, also Kepler’s 3rd law is of geometric origin and can be derived from Gauss’s flux theorem in 3D-space within basic scale considerations. It applies to all conservative fields which decrease with the square of the distance, similar to the geometric dilution of the intensity of light into 3D-space.

The theoretical reduction of gravity to an acceleration enables the orbital motion to be identified with free fall. Orbital and rotational motions are periodic. So is free fall. Only the aggregate state of the planet prevents the free fall from becoming a damped oscillation. Considering gravity acting with the speed of light c , we can express gravity in units of time. For instance, Earth’s surface gravity $g_{\text{Earth}} = 9.81 \text{ m/s}^2$ corresponds with an oscillation period of 355 days that is quite close to Earth’s orbital period:

$$T_{\text{Earth}} = \frac{c}{g_{\text{Earth}}} = \frac{299792458 \text{ m/s}}{9.81 \text{ m/s}^2} = 355 \text{ d}.$$

At an altitude of 100 km above sea level, Earth’s gravity reduces down to 9.51 m/s^2 that corresponds with the orbital period of 365.25 days. In a series of experiments we demonstrated [23] that inside of finite spatial configurations which boundaries coincide with equipotential surfaces of the Fundamental Field (fig. 2), gravity acceleration reduces locally by $0.3 g$ down to 9.51 m/s^2 .

The surface gravity $g_{\text{Sun}} = 274 \text{ m/s}^2$ of the Sun corresponds with an oscillation period of 12.7 days that is the first harmonic of its equatorial period 25.4 days of rotation. Similar coincidences are valid for the surface gravities of Mercury, Venus, Mars and even for Saturn and Jupiter. Although the definition of a planet’s surface is conventional (especially in the case of gas giants), all these coincidences suggest the existence of an underlying connection of the gravity of a celestial body with its *own* orbital and rotational motions. Despite the rich history of crucial discoveries in astronomy and

astrophysics and the development of sophisticated theories of gravitation, the distribution of stable orbits in the solar system remains to be little understood. In this context, the discovery of Johann Daniel Titius (1766) is even more remarkable. He found that the sequence of the planetary semi-major axes can be approximated by the exponential term:

$$a_n = 0.4 + 0.3 \cdot 2^n,$$

where the index n is $-\infty$ for Mercury, 0 for Venus, 1 for the Earth, 2 for Mars etc. Based on this idea, Johann Elert Bode, in 1772, first suggested that an undiscovered planet could exist between the orbits of Mars and Jupiter. William Herschel's discovery of Uranus in 1781 near the predicted distance 19.6 AU for the next body beyond Saturn increased faith in the law of Titius and Bode. In 1801, near the predicted for $n = 3$ distance 2.8 AU from Sun, Giuseppe Piazzi discovered the planetoid Ceres and the Franz Xaver von Zach group found further large asteroids.

In 1968, Stanley Dermott [24] found a similar progression for the major satellites of Jupiter, Saturn and Uranus. Nevertheless, at last, the hypothesis of Titius and Bode was discarded after it failed as a predictor of Neptune's orbit.

Surprisingly, recent astronomical research [25] suggests that exoplanetary systems follow Titius-Bode-like laws. Raw statistics from exoplanetary orbits indicate the exponential increase of semi-major axes as function of planetary index. It has been shown [2] that many exoplanetary systems follow an exponential progression of the form

$$a_n = a_0 + e^{bn}$$

with $n = 0, 1, 2, \dots$; a_0 and b are constants to be determined for each system. Since its formulation, the Titius-Bode law has proved to be highly predictive, although its physical origin remains largely unclear.

Not only the distribution of stable orbits, but also the origin of the configuration of gravity fields in the solar system remains disputed. Furthermore, there is no known law concerning the rotation of celestial bodies besides conservation of the angular momentum [26] that they retain from the protoplanetary disks, so that the final distribution of the rotational periods appears as to be accidental.

In this article we demonstrate that the rotational and orbital periods of the planets, planetoids and large moons of the solar system as well as their gravitational constants approximate numeric attractors corresponding with the transcendental frequency ratios of scale-invariant eigenstates in chain systems of oscillating protons and electrons. The claims of our model we verify also on orbital periods of exoplanets and the gravitational constants of their stars.

Methods

In [27] we have shown that the difference between rational, irrational algebraic and transcendental numbers is not only a

mathematical task, but it is also an essential aspect of stability in complex dynamic systems. For instance, integer frequency ratios provide resonance interaction that can destabilize a system [28]. Actually, it is transcendental numbers that define the preferred ratios of quantities which avoid destabilizing resonance interaction [29]. In this way, transcendental ratios of quantities sustain the lasting stability of periodic processes in complex dynamic systems. With reference to the evolution of a planetary system and its stability, we may therefore expect that the ratio of any two orbital periods should finally approximate a transcendental number.

Among all transcendental numbers, Euler's number $e = 2.71828\dots$ is unique, because its real power function e^x coincides with its own derivatives. In the consequence, Euler's number allows inhibiting resonance interaction regarding any interacting periodic processes and their derivatives. Because of this unique property of Euler's number, complex dynamic systems tend to establish relations of quantities that coincide with values of the natural exponential function e^x for integer and rational exponents x .

Therefore, we expect that periodic processes in real systems prefer frequency ratios close to Euler's number and its rational powers. Consequently, the logarithms of their frequency ratios should be close to integer $0, \pm 1, \pm 2, \dots$ or rational values $\pm 1/2, \pm 1/3, \pm 1/4, \dots$. In [30] we exemplified our hypothesis in particle physics, astrophysics, cosmology, geophysics, biophysics and engineering.

Based on this hypothesis, we introduced a fractal model of matter [31] as a chain system of harmonic quantum oscillators and could show the evidence of this model for all known hadrons, mesons, leptons and bosons as well. In [32] we have shown that the set of stable eigenstates in such systems is fractal and can be described by finite continued fractions:

$$\mathcal{F}_{jk} = \ln(\omega_{jk}/\omega_{00}) = \langle n_{j0}; n_{j1}, n_{j2}, \dots, n_{jk} \rangle, \quad (1)$$

where ω_{jk} is the set of angular eigenfrequencies and ω_{00} is the fundamental frequency of the set. The denominators are integer: $n_{j0}, n_{j1}, n_{j2}, \dots, n_{jk} \in \mathbb{Z}$. The cardinality $j \in \mathbb{N}$ of the set and the number $k \in \mathbb{N}$ of layers are finite. In the canonical form, all numerators equal 1. We use angle brackets for continued fractions.

Any finite continued fraction represents a rational number [33]. Therefore, the ratios ω_{jk}/ω_{00} of eigenfrequencies are always irrational, because for rational exponents the natural exponential function is transcendental [34]. This circumstance provides for lasting stability of those eigenstates of a chain system of harmonic oscillators because it prevents resonance interaction [35] between the elements of the system.

The distribution density of stable eigenstates reaches local maxima near reciprocal integers $\pm 1/2, \pm 1/3, \pm 1/4, \dots$ that are attractor points (fig. 1) in the fractal set \mathcal{F}_{jk} of natural logarithms. Integer logarithms $0, \pm 1, \pm 2, \dots$ represent the most stable eigenstates (main attractors).

In the case of harmonic quantum oscillators, the continued fractions \mathcal{F}_{jk} define not only fractal sets of natural angular frequencies ω_{jk} , angular accelerations $a_{jk} = c \cdot \omega_{jk}$, oscillation periods $\tau_{jk} = 1/\omega_{jk}$ and wavelengths $\lambda_{jk} = c/\omega_{jk}$ of the chain system, but also fractal sets of energies $E_{jk} = \hbar \cdot \omega_{jk}$ and masses $m_{jk} = E_{jk}/c^2$ which correspond with the eigenstates of the system. For this reason, we call the continued fraction \mathcal{F}_{jk} the *Fundamental Fractal* of stable eigenstates in chain systems of harmonic quantum oscillators.



Fig. 1: The distribution of stable eigenvalues of \mathcal{F}_{jk} for $k = 1$ (above) and for $k = 2$ (below) in the range $-1 \leq \mathcal{F}_{jk} \leq 1$.

The spatio-temporal projection of the Fundamental Fractal \mathcal{F}_{jk} of stable eigenstates is a fractal scalar field of transcendental attractors, the *Fundamental Field* [36].

The connection between the spatial and temporal projections of the Fundamental Fractal is given by the speed of light $c = 299792458$ m/s. The constancy of c makes both projections isomorphic, so that there is no arithmetic or geometric difference. Only the units of measurement are different.

Figure 2 shows the linear 2D-projection $\exp(\mathcal{F}_{jk})$ of the first layer of the Fundamental Field

$$\mathcal{F}_{j1} = \langle n_{j0}; n_{j1} \rangle = n_{j0} + \frac{1}{n_{j1}}$$

in the interval $-1 < \mathcal{F}_{j1} < 1$. The upper part of figure 1 shows the same interval in the logarithmic representation. The Fundamental Field is topologically 3-dimensional, a fractal set of embedded spheric equipotential surfaces. The logarithmic potential difference defines a gradient directed to the center of the field that causes a central force of attraction. Because of the fractal logarithmic hyperbolic metric of the field, every equipotential surface is an attractor. The scalar potential difference $\Delta\mathcal{F}$ of sequent equipotential surfaces at a given layer k is defined by the difference of continued fractions (1):

$$\begin{aligned} \Delta\mathcal{F} &= \mathcal{F}(j,k) - \mathcal{F}(j+1,k) = \\ &= \langle n_{j0}; n_{j1}, n_{j2}, \dots, n_{jk} \rangle - \langle n_{j0}; n_{j1}, n_{j2}, \dots, n_{j+1,k} \rangle. \end{aligned}$$

For instance, at the first layer $k=1$, the potential differences have the form:

$$\Delta\mathcal{F} = \frac{1}{n_{j1}} - \frac{1}{n_{j1} + 1} = \frac{1}{n_{j1}^2 + n_{j1}}.$$

Therefore, the potential difference between sequent equipotential surfaces at any given layer $k + 1$ decreases parabolically, approximating zero near an equipotential surface of the layer k . This is why any equipotential surface is an attractor where potential differences decrease and processes can gain stability. Main attractors at the layer $k = 0$ correspond with

integer logarithms, subattractors at deeper layers $k > 0$ correspond with rational logarithms.

The Fundamental Field is of pure arithmetical origin, and there is no particular physical mechanism required as field source. It is all about transcendental ratios of frequencies [29] that inhibit destabilizing resonance. In this way, the Fundamental Field concerns all repetitive processes which share at least one characteristic — the frequency. Therefore, we postulate the universality of the Fundamental Field that affects any type of physical interaction, regardless of its complexity.

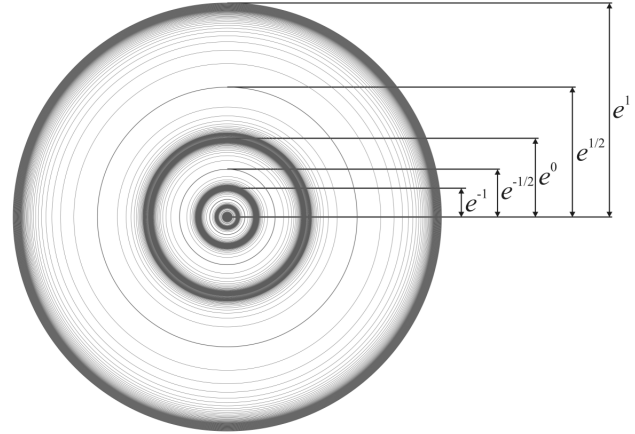


Fig. 2: The equipotential surfaces of the Fundamental Field in the linear 2D-projection for $k = 1$.

In fact, scale relations in particle physics [31, 37, 38], nuclear physics [39, 40] and astrophysics [4] obey the same Fundamental Fractal (1), without any additional or particular settings. The proton-to-electron rest energy ratio approximates the first layer of the Fundamental Fractal that could explain their exceptional stability [30]. The life-spans of the proton and electron top everything that is measurable, exceeding 10^{29} years [41].

PROPERTY	ELECTRON	PROTON
$E = mc^2$	0.5109989461(31) MeV	938.2720813(58) MeV
$\omega = E/\hbar$	$7.76344 \cdot 10^{20}$ Hz	$1.42549 \cdot 10^{24}$ Hz
$\tau = 1/\omega$	$1.28809 \cdot 10^{-21}$ s	$7.01515 \cdot 10^{-25}$ s
$\lambda = c/\omega$	$3.86159 \cdot 10^{-13}$ m	$2.10309 \cdot 10^{-16}$ m

Table 1: The basic set of the physical properties of the electron and proton. Data from Particle Data Group [41]. Frequencies, oscillation periods and wavelengths are calculated.

These unique properties of the electron and proton predestinate their physical characteristics as fundamental units. Table 1 shows the basic set of electron and proton units that can be considered as a fundamental metrology (c is the speed of light in a vacuum, \hbar is the Planck constant). In [32] was

shown that the fundamental metrology (tab. 1) is completely compatible with Planck units [42]. Originally proposed in 1899 by Max Planck, these units are also known as natural units, because the origin of their definition comes only from properties of nature and not from any human construct. Max Planck wrote [43] that these units, “regardless of any particular bodies or substances, retain their importance for all times and for all cultures, including alien and non-human, and can therefore be called natural units of measurement”. Planck units reflect the characteristics of space-time.

We hypothesize that scale invariance according the Fundamental Fractal (1) calibrated on the physical properties of the proton and electron is a universal characteristic of organized matter and criterion of stability. This hypothesis we have called *Global Scaling* [30].

On this background, atoms and molecules emerge as stable eigenstates in fractal chain systems of harmonically oscillating protons and electrons. Andreas Ries [38] demonstrated that this model allows for the prediction of the most abundant isotope of a given chemical element.

In [44] we applied the Fundamental Fractal (1) to macroscopic scales interpreting gravity as attractor effect of its stable eigenstates. Indeed, the orbital and rotational periods of planets, planetoids and large moons of the solar system correspond with attractors of electron and proton stability [32]. This is valid also for the planets [30] of the systems Trappist 1 and Kepler 20. Planetary and lunar orbits [4] correspond with equipotential surfaces of the Fundamental Field, as well as the metric characteristics of stratification layers in planetary atmospheres [45]. In [36] we demonstrated that the Fundamental Field (fig. 2) in the interval of the main attractors $\langle 49 \rangle \leq \mathcal{F} \leq \langle 52 \rangle$ of proton stability reproduces the 2D profile of the Earth’s interior confirmed by seismic exploration.

Results

We will show now that the orbital and rotational periods of planets, planetoids and moons as well as their gravity accelerations approximate stable eigenstates of our model of matter as fractal chain system of oscillating protons and electrons, described by the Fundamental Fractal.

In accordance with the equation (1), we calculate the natural logarithm of the ratio of the measured value to the corresponding electron or proton unit taken from table 1. For instance, the orbital period of Jupiter T_O (Jupiter) = 4332.59 days = $3.7434 \cdot 10^8$ seconds [46] matches the main attractor $\mathcal{F}\langle 66 \rangle$ of *electron* stability:

$$\ln\left(\frac{T_O(\text{Jupiter})}{2\pi \cdot \tau_e}\right) = \ln\left(\frac{3.7434 \cdot 10^8 \text{ s}}{2\pi \cdot 1.28809 \cdot 10^{-21} \text{ s}}\right) = 66.00.$$

In contrast to orbital motion, rotation is an angular motion, so that the proton or electron angular oscillation periods are applied as units. The rotation period $T_R(\text{Ceres}) = 9$ hours = 32400 seconds of Ceres, the largest body of the main asteroid

belt, matches the main attractor $\mathcal{F}\langle 66 \rangle$ of *proton* stability:

$$\ln\left(\frac{T_R(\text{Ceres})}{\tau_p}\right) = \ln\left(\frac{32400 \text{ s}}{7.01515 \cdot 10^{-25} \text{ s}}\right) = 66.00.$$

Table 3 gives an overview of the orbital and rotational periods as well as the gravitational constants of the planets including the planetoid Ceres and large moons.

Within our model, the approximation level of an attractor of stability indicates evolutionary trends. For instance, Venus’ OE2 = 63.04 indicates that the orbital period of the Morning star must slightly decrease for reaching the center of the main attractor $\mathcal{F}\langle 63 \rangle$. On the contrary, Moon’s OE2 = 60.94 indicates that its orbital period must still increase for reaching the center of the main attractor $\mathcal{F}\langle 61 \rangle$. Actually, exactly this is observed [47]. As well, Uranus’ OE2 = 67.96 let us expect an increase of its orbital period in order to reach the main attractor $\mathcal{F}\langle 68 \rangle$. Mercury’s OE1 = 63.94 indicates that in future it could overcome the current tidal 3/2 locking by reaching the main attractor $\mathcal{F}\langle 64 \rangle$ of electron stability. Mercury’s RP1 = 71.05 indicates that its rotation must speed up slightly [26] in order to reach the attractor $\mathcal{F}\langle 71 \rangle$ of proton stability. Earth’s RP1 = 66.98 indicates that our planet must slow its rotation by 24 minutes per turn in order to reach the main attractor $\mathcal{F}\langle 67 \rangle$.

Despite conservation of angular momentum [26], there is no known law concerning the rotation of celestial bodies. The more remarkable is the correspondence of the rotation periods of planets, planetoids and large moons with attractors of the Fundamental Fractal (1) as shown in table 3.

For instance, Mars, Ceres and Jupiter have reached the main attractor $\mathcal{F}\langle 66 \rangle$ in quite different way. In the case of Mars and Jupiter, the attractor $\mathcal{F}\langle 66 \rangle$ stabilizes the orbital period T_O . In the case of the planetoid Ceres, the same attractor $\mathcal{F}\langle 66 \rangle$ stabilizes the period of rotation T_R . Actually, the difference lays in the reference units. In the case of Jupiter’s orbital period, the reference unit is the oscillation period of the electron $2\pi\tau_e$; in the case of Mars, it is the angular oscillation period of the electron τ_e , and in the case of the rotational period of Ceres, it is the angular oscillation period of the proton τ_p . Now we can write down the following relations:

$$T_O(\text{Jupiter}) = 2\pi \cdot T_O(\text{Mars}),$$

$$T_O(\text{Mars}) = \frac{\tau_e}{\tau_p} \cdot T_R(\text{Ceres}).$$

The complete (polar) rotational period of the Sun approximates the main attractor $\mathcal{F}\langle 63 \rangle$ of electron stability:

$$\ln\left(\frac{T_R(\text{Sun})}{\tau_e}\right) = 63.01.$$

The orbital period of Venus approximates the same attractor $\mathcal{F}\langle 63 \rangle$, as table 3 shows. Consequently, the scaling factor 2π

connects the orbital period of Venus with the rotational period of the Sun:

$$T_O(\text{Venus}) = 2\pi \cdot T_R(\text{Sun}).$$

Archimedes' number $\pi = 3.14159\dots$ is transcendental and therefore, it does not violate the principle of avoiding destabilizing resonance. Needless to say that these relations cannot be derived from Kepler's laws or Newton's law of gravitation. The proton-to-electron ratio (tab. 1) approximates the seventh power of Euler's number and its square root:

$$\ln\left(\frac{\omega_p}{\omega_e}\right) = \ln\left(\frac{1.42549 \cdot 10^{24} \text{ Hz}}{7.76344 \cdot 10^{20} \text{ Hz}}\right) \approx 7 + \frac{1}{2} = \langle 7; 2 \rangle.$$

In the consequence of this potential difference of the proton relative to the electron, the scaling factor $\sqrt{e} = 1.64872\dots$ connects attractors of proton stability with similar attractors of electron stability in alternating sequence. The following Diophantine equation describes the correspondence of proton calibrated attractors n_p with electron calibrated attractors n_e . Non considering the signature, only three pairs (n_p, n_e) of integers are solutions to this equation: (3, 6), (4, 4), (6, 3).

$$\frac{1}{n_p} + \frac{1}{n_e} = \frac{1}{2}.$$

Figure 3 demonstrates this situation on the first layer of the Fundamental Fractal (1). Both, the attractors of proton and electron stability are represented at the first layer, so we can see clearly that among the integer or half, only the attractors $\pm 1/3, \pm 1/4$ and $\pm 1/6$ are common. In these attractors, proton stability is supported by electron stability and vice versa, so we expect that they are preferred in real systems.



Fig. 3: The distribution of the attractors of proton (bottom) stability in the range $-1 < \mathcal{F} < 1$ of the attractors of electron (top) stability. Natural logarithmic representation.

Figure 4 shows the distribution of the number of exoplanets with orbital periods in the range $5 \text{ d} < T_O < 24 \text{ d}$ that corresponds with the range of logarithms $59.2 < \ln(T_O/2\pi\tau_e) < 60.8$ on the horizontal axis. According with table 1, τ_e is the electron angular oscillation period. The histogram contains data of 1430 exoplanets and shows clearly the maximum corresponding with the main attractor $\mathcal{F}\langle 60 \rangle$. Other maxima correspond with the attractors $\mathcal{F}\langle 59; 2 \rangle$ and $\mathcal{F}\langle 60; 2 \rangle$; even the subattractors $\mathcal{F}\langle 60; -4 \rangle$ and $\mathcal{F}\langle 60; 4 \rangle$ can be distinguished.

The histogram evidences that the majority of the analyzed 1430 exoplanets [48] prefer orbital periods close to 10–11 days corresponding with the main attractor $\mathcal{F}\langle 60 \rangle$, as well as periods close to 6–7 days or close to 17–18 days corresponding with the attractors $\mathcal{F}\langle 59; 2 \rangle$ and $\mathcal{F}\langle 60; 2 \rangle$. Because of the logarithm $7+1/2$ of the proton-to-electron ratio, the attractors

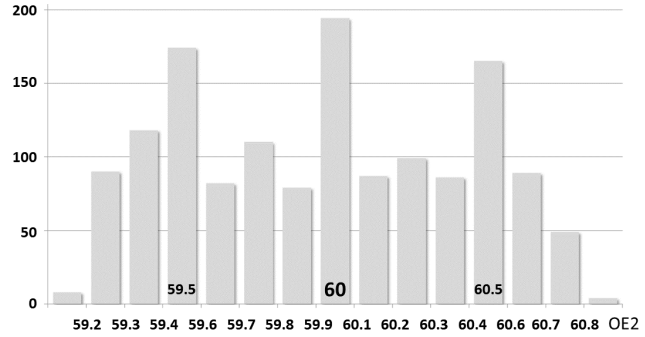


Fig. 4: The histogram shows the distribution of the number of exoplanets with orbital periods in the range $5 \text{ d} < T_O < 24 \text{ d}$. The logarithms $\text{OE2} = \ln(T_O/2\pi\tau_e)$ are on the horizontal axis. Corresponding with table 1, τ_e is the electron angular oscillation period. Data of 1430 exoplanets taken from [48].

$\mathcal{F}\langle 59; 2 \rangle$ and $\mathcal{F}\langle 60; 2 \rangle$ of electron stability are actually the main attractors $\mathcal{F}\langle 67 \rangle$ and $\mathcal{F}\langle 68 \rangle$ of proton stability.

Now we can also explain the origin of the Titius-Bode law. The OE2 column in tab. 3 shows that the orbital periods of Ceres, Jupiter, Saturn and Uranus approximate the sequence of the main attractors $\mathcal{F} = \langle 65 \rangle, \langle 66 \rangle, \langle 67 \rangle$ and $\langle 68 \rangle$ of electron stability. The ratio of main attractors equals Euler's number $e = 2.71828\dots$. Considering Kepler's third law, from this directly follows that the ratio of the semi-major axes of Ceres, Jupiter, Saturn and Uranus approximates the cube root of the square of Euler's number $e^{2/3} = 1.9477\dots$. This is why the Titius-Bode law approximates the exponential function 2^n . However, not all orbital periods approximate main attractors. The Earth-Venus orbital period ratio approximates the square root of Euler's number. Consequently, the ratio of their semi-major axes approximates the cube root of Euler's number $e^{1/3} = 1.3956\dots$. The same is valid for Umbriel and Ariel, the moons of Uranus. The Neptune-Uranus orbital period ratio approximates $e^{2/3}$. Consequently, the ratio of their semi-major axes approximates $e^{4/9} = 1.5596\dots$

The eigenvalues of \mathcal{F} are transcendental, and their distribution (1) is logarithmically fractal. This is why Titius-Bode-like equations cannot deliver a general and complete model of an orbital system.

Among the orbital and rotational periods, tab. 3 shows that also the gravitational constants μ obey the Fundamental Fractal (1) approximating main attractors and the preferred subattractors as shown in fig. 3.

In accordance with [46], surface gravities g are given for a distance from the center of the celestial body that coincides with the radius of the solid or liquid surface, without consideration of the centrifugal effects of rotation. For gas giants such as Jupiter, Saturn, Uranus, and Neptune, where the surfaces are deep in the atmosphere and the radius is not known, the surface gravity is given at the 1 bar pressure level in the atmosphere. In this way, any surface gravity is given for an individual distance from the local center of gravitation.

Earth’s surface gravity corresponds to the equatorial radius at sea level 6378 km, and the surface gravity of Uranus corresponds to its equatorial radius of 25559 km where the atmospheric pressure equals 1 bar. Although the surface gravities on Venus and Uranus are identical equal 8.87 m/s^2 , this does not mean that they indicate comparable gravitational fields. Therefore, we cannot use the surface gravity accelerations for comparison, but only the gravitational constants μ .

STAR	$\mu, \text{ m}^3/\text{s}^2$	MP	\mathcal{F}	MP - \mathcal{F}
Trappist 1	$1.1976 \cdot 10^{19}$	40.99	$\langle 41 \rangle$	-0.01
Proxima Cent	$1.5725 \cdot 10^{19}$	41.26	$\langle 41; 4 \rangle$	0.01
Gliese 1061	$1.6966 \cdot 10^{19}$	41.34	$\langle 41; 3 \rangle$	0.01
Barnard’s star	$2.6154 \cdot 10^{19}$	41.77	$\langle 42; -4 \rangle$	0.02
Struve 2398 B	$3.7765 \cdot 10^{19}$	42.14	$\langle 42; 6 \rangle$	-0.02
Gliese 876	$4.2851 \cdot 10^{19}$	42.27	$\langle 42; 4 \rangle$	0.02
Lacaille 9352	$6.4378 \cdot 10^{19}$	42.67	$\langle 43; -3 \rangle$	0.00
Tau Ceti	$1.0414 \cdot 10^{20}$	43.15	$\langle 43; 6 \rangle$	-0.01
HD 69830	$1.1402 \cdot 10^{20}$	43.24	$\langle 43; 4 \rangle$	-0.01
55 Cancri	$1.2480 \cdot 10^{20}$	43.33	$\langle 43; 3 \rangle$	0.00
Upsilon Andro	$1.7598 \cdot 10^{20}$	43.68	$\langle 44; -3 \rangle$	0.01

Table 2: The gravitational constants μ of some stars calculated from data [48] of orbital periods and semi-major axes of their planets. $MP = \ln(\mu/\lambda_p^3\omega_p^2)$. Corresponding with tab. 1, λ_p is the proton angular wavelength and ω_p is the proton angular frequency. Continued fractions (1) of the Fundamental Fractal \mathcal{F} are given in angle brackets.

Table 3 shows that the gravitational constants μ of Pluto, Neptune, Jupiter, Mars and Venus approximate main attractors $\mathcal{F}=\langle n_0 \rangle$ of electron stability. The gravitational constants of the other planets and planetoids of the solar system approximate the rational subattractors $\mathcal{F}=\langle n_0 \pm 1/2 \rangle$, $\langle n_0 \pm 1/3 \rangle$, $\langle n_0 \pm 1/4 \rangle$ or $\langle n_0 \pm 1/6 \rangle$. As well, the gravitational constants of the large moons of Jupiter, Saturn, Uranus and Neptune approximate main attractors of electron and proton stability and the same rational subattractors. This is valid also for exoplanetary systems. Table 2 shows the gravitational constants μ of some near stars calculated from data [48] of the orbital periods and semi-major axes of their planets.

Conclusion

Perhaps, the conventional paradigm of physical interaction should be completed by the principle of avoiding those interactions that potentially can destabilize a system.

Admittedly, the principle of minimum action is an essential part of theoretical physics at least since Pierre de Fermat (1662) and Pierre Louis Moreau de Maupertuis (1741),

Joseph-Louis Lagrange (1788) and William Rowan Hamilton (1834) applied in the Euler – Lagrange equations of motion.

The novelty of our solution we see in the purely numerical approach that rediscovers Euler’s number, its integer powers and roots as attractors of transcendental numbers. Approximating transcendental ratios of quantities defined by integer and rational natural logarithms, complex dynamic systems can avoid destabilizing resonance interactions between their elements and gain lasting stability. As we have shown in this paper, planetary systems make extensive use of this solution.

Finally, we can explain why Jupiter’s orbital period equals 4332.59 days: With this orbital period, Jupiter occupies the main equipotential surface $\mathcal{F}=\langle 66 \rangle$ of the Fundamental Field of transcendental attractors and in this way, Jupiter avoids destabilizing resonance interactions with the orbital motions of other planets and gains lasting stability of its own orbital motion. In other words, there is a fractal scalar field of transcendental temporal attractors corresponding with integer and rational powers of Euler’s number. One of these attractors is $\mathcal{F}=\langle 66 \rangle$, and it has materialized as a stable orbital period in the solar system among the attractors $\mathcal{F} = \langle 62 \rangle, \langle 63 \rangle, \langle 64 \rangle, \langle 65 \rangle, \langle 67 \rangle, \langle 68 \rangle, \langle 69 \rangle$ and their subattractors. Smaller attractors $\mathcal{F} = \langle 58 \rangle, \langle 59 \rangle, \langle 60 \rangle$ and $\langle 61 \rangle$ and their subattractors define stable orbital periods in moon systems and in the majority of the discovered so far exoplanetary systems.

Naturally, the Fundamental Field \mathcal{F} of transcendental attractors does not materialize in the scale of planetary systems only. At subatomic scale, it defines the proton-to-electron ratio and in this way, allows the formation of stable atoms and complex matter. At planetary scale, now we can distinguish attractors of electron stability and attractors of proton stability. While the attractors of electron stability define stable orbital periods, the attractors of proton stability define stable rotational periods. For instance, the attractor $\mathcal{F}=\langle 66 \rangle$ of *electron* stability defines the orbital period of Jupiter, and the same attractor $\mathcal{F}=\langle 66 \rangle$ of *proton* stability defines the rotational period of Mars. In this way, the law behind the distribution of stable orbital and rotational periods is the same Fundamental Field of transcendental attractors.

Interpreting gravity in terms of frequency, we did demonstrate that the distribution of gravity in the solar system is not accidental, but obeys the same Fundamental Field \mathcal{F} . As well, the gravitational constants μ of extrasolar systems obey the logarithmically fractal metric (1) of \mathcal{F} . This circumstance let us suppose that even entire planetary systems prefer avoiding destabilizing resonance interactions between them.

Acknowledgements

The author is grateful to Simon Shnoll, Viktor Panchelyuga, Valery Kolombet, Oleg Kalinin, Viktor Bart, Andreas Ries, Michael Kauderer, Ulrike Granögger and Leili Khosravi for valuable discussions.

Submitted on January 7, 2021

Body	T_O , d	OE1	\mathcal{F}	OE2	\mathcal{F}	T_R , h	RP1	\mathcal{F}	RP2	\mathcal{F}	μ , m^3/s^2	ME	\mathcal{F}
Eris	204199.00	71.69	(72; -3)	69.86	(70; -6)	349.44	69.66	(70; -3)	67.82	(68; -6)	$1.10800 \cdot 10^{12}$	17.28	(17; 4)
Pluto	90560.09	70.88	(71; -6)	69.04	(69)	153.29	68.84	(69; -6)	67.00	(67)	$8.62000 \cdot 10^{11}$	17.03	(17)
Neptune	60193.20	70.47	(70; 2)	68.64	(69; -3)	16.11	66.58	(66; 2)	64.75	(65; -4)	$6.83653 \cdot 10^{15}$	26.01	(26)
Uranus	30688.49	69.80	(70; -6)	67.96	(68)	17.24	66.65	(67; -3)	64.81	(65; -6)	$5.79394 \cdot 10^{15}$	25.84	(26; -6)
Saturn	10759.21	68.75	(69; -4)	66.91	(67)	10.56	66.16	(66; 6)	64.32	(64; 3)	$3.79312 \cdot 10^{16}$	27.72	(28; -4)
Jupiter	4332.60	67.84	(68; -6)	66.00	(66)	9.93	66.10	(66; 6)	64.26	(64; 3)	$1.26687 \cdot 10^{17}$	28.93	(29)
Ceres	1683.80	66.90	(67; -6)	65.06	(65)	9.00	66.00	(66)	64.16	(64; 6)	$6.26274 \cdot 10^{10}$	14.41	(14; 2)
Mars	686.97	66.00	(66)	64.16	(64; 6)	24.62	67.01	(67)	65.17	(65; 6)	$4.28284 \cdot 10^{13}$	20.93	(21)
Earth	365.25	65.37	(65; 3)	63.53	(63; 2)	24.00	66.98	(67)	65.15	(65; 6)	$3.98600 \cdot 10^{14}$	23.16	(23; 6)
Venus	224.70	64.88	(65; -6)	63.04	(63)	243.03	72.48	(72; 2)	70.64	(71; -3)	$3.24859 \cdot 10^{14}$	22.96	(23)
Mercury	87.97	63.94	(64)	62.11	(62; 6)	58.65	71.05	(71)	69.22	(69; 6)	$2.20320 \cdot 10^{13}$	20.27	(20; 4)
Moon	27.32	62.78	(63; -6)	60.94	(61)	sync	70.29	(70; 3)	68.45	(68; 2)	$4.90487 \cdot 10^{12}$	18.77	(19; -4)
Callisto	16.69	62.28	(62; 3)	60.44	(60; 2)	sync	69.80	(70; -6)	67.96	(68)	$7.17929 \cdot 10^{12}$	19.15	(19; 6)
Ganymede	7.15	61.44	(61; 2)	59.60	(60; -3)	sync	68.95	(69)	67.11	(67; 6)	$9.88783 \cdot 10^{12}$	19.47	(19; 2)
Europa	3.55	60.74	(61; -4)	58.90	(59)	sync	68.25	(68; 4)	66.41	(66; 2)	$3.20274 \cdot 10^{12}$	18.34	(18; 3)
Io	1.77	60.04	(60)	58.20	(58; 6)	sync	67.55	(67; 2)	65.72	(66; -3)	$5.95992 \cdot 10^{12}$	18.96	(19)
Iapetus	79.32	63.84	(64; -6)	62.00	(62)	sync	71.36	(71; 3)	69.52	(69; 2)	$1.20500 \cdot 10^{11}$	15.06	(15)
Titan	15.95	62.24	(62; 4)	60.40	(60; 2)	sync	69.75	(70; -4)	67.91	(68)	$8.96273 \cdot 10^{12}$	19.37	(19; 3)
Rhea	4.52	60.98	(61)	59.14	(59; 6)	sync	68.49	(69; 2)	66.65	(67; -3)	$1.54000 \cdot 10^{11}$	15.31	(15; 3)
Dione	2.74	60.47	(60; 2)	58.64	(59; -3)	sync	67.99	(68)	66.15	(66; 6)	$7.10000 \cdot 10^{10}$	14.53	(14; 2)
Tethys	1.89	60.10	(60; 6)	58.27	(58; 3)	sync	67.62	(68; -3)	65.78	(66; -6)	$4.12000 \cdot 10^{10}$	13.99	(14)
Enceladus	1.37	59.78	(60; -6)	57.94	(58)	sync	67.30	(67; 3)	65.46	(65; 2)	$7.20000 \cdot 10^9$	12.24	(12; 4)
Mimas	0.94	59.41	(59; 3)	57.57	(57; 2)	sync	66.92	(67)	65.09	(65)	$2.50000 \cdot 10^9$	11.18	(11; 6)
Oberon	13.46	62.07	(62)	60.23	(60; 6)	sync	69.58	(69; 2)	67.75	(68; -4)	$1.93000 \cdot 10^{11}$	15.53	(15; 2)
Titania	8.71	61.63	(62; -3)	59.79	(60; -6)	sync	69.15	(69; 6)	67.31	(67; 3)	$2.20000 \cdot 10^{11}$	15.66	(16; -3)
Umbriel	4.14	60.89	(61; -6)	59.05	(59)	sync	68.40	(68; 3)	66.57	(66; 2)	$8.95000 \cdot 10^{10}$	14.76	(15; -4)
Ariel	2.52	60.39	(60; 3)	58.55	(58; 2)	sync	67.91	(68; -6)	66.07	(66)	$7.88000 \cdot 10^{10}$	14.64	(15; -3)
Miranda	1.41	59.81	(60; -6)	57.98	(58)	sync	67.33	(67; 3)	65.49	(65; 2)	$4.00000 \cdot 10^9$	11.65	(12; -3)
Triton	5.88	61.24	(61; 4)	59.40	(59; 2)	sync	68.75	(69; -4)	66.92	(67)	$1.42689 \cdot 10^{12}$	17.53	(17; 2)

Table 3: The sidereal orbital periods T_O , rotational periods T_R and gravitational constants μ of the planets, planetoids and large moons of the solar system. OE1 = $\ln(T_O/\tau_e)$, OE2 = $\ln(T_O/2\pi\tau_e)$, RP1 = $\ln(T_R/\tau_p)$, RP2 = $\ln(T_R/2\pi\tau_p)$, ME = $\ln(\mu/\lambda_e^3\omega_e^2)$. Corresponding with tab. 1, τ_e is the *electron* angular oscillation period, τ_p is the *proton* angular oscillation period, λ_e is the *electron* angular wavelength and ω_e is the *electron* angular frequency. The continued fractions (1) of the Fundamental Fractal \mathcal{F} are given in angle brackets. Although some data is shown with two decimals only, for calculating the logarithms, high precision data [46, 49–51] were used.

References

1. Verlinde E. On the origin of gravity and the laws of Newton. *arXiv:1001.0785v1 [hep-th]* 6 Jan 2010.
2. Lara P., Cordero-Tercero G., Allen Ch. The reliability of the Titius-Bode relation and its implications for the search for exoplanets. *arXiv:2003.05121v1 [astro-ph.EP]* 11 Mar 2020.
3. Brookes C. J. On the prediction of Neptune. Provided by the NASA Astrophysics Data System. *Kluwer Academic Publishers*, (1970).
4. Müller H. Global Scaling of Planetary Systems. *Progress in Physics*, 2018, v. 14, 99–105.
5. Gillon M. et al. Seven temperate terrestrial planets around the nearby ultracool dwarf star TRAPPIST-1. *Nature*, 21360, 2017.
6. Hand E. Kepler discovers first Earth-sized exoplanets. *Nature*, 9688, 2011.
7. Turyshev S. G., Toth V. T. The Puzzle of the Flyby Anomaly. *arXiv:0907.4184v1 [gr-qc]* 23 Jul 2009.
8. Schlamminger S. et al. Test of the Equivalence Principle Using a Rotating Torsion Balance. *arXiv:0712.0607v1 [gr-qc]* 4 Dec 2007.
9. Janiak A. Newton and the Reality of Force. *Journal of the History of Philosophy*, vol. 45, Nr. 1 (2007) 127–147.
10. Gillies G. T. The Newtonian gravitational constant: recent measurements and related studies. *Rep. Prog. Phys.*, vol. 60, 151–225, (1997).
11. Stacey F. D., Tuck G. J. Geophysical evidence for non-newtonian gravity. *Nature*, v. 292, pp. 230–232, (1981).
12. Miller A. H. Gravity and Isostasy. *Journal of the Royal Astronomical Society of Canada*, vol. 20, p. 327, (1926).
13. Battaglia M., Gottsmann J., Carbone D., Fernández J. 4D volcano gravimetry. *Geophysics*, vol.73, Nr. 6, (2008).
14. Van Camp M. Measuring seismic normal modes with the GWR C021 superconducting gravimeter. *Physics of the Earth and Planetary Interiors*, vol. 116, pp. 81–92, (1999).
15. Heki K., Matsuo K. Coseismic gravity changes of the 2010 earthquake in central Chile from satellite gravimetry. *Geophysical Research Letters*, vol. 37, L24306, (2010).
16. Dziewonski A. M., Anderson D. L. Preliminary reference Earth model. *Physics of the Earth and Planetary Interiors*, vol. 25, 297–356, (1981).
17. Stacey F. D. et al. Constraint on the planetary scale value of the Newtonian gravitational constant from the gravity profile within a mine. *Phys. Rev. D* 23, 1683, (1981).
18. Holding S. C., Stacey F. D., Tuck G. J. Gravity in mines. An investigation of Newton's law. *Phys. Rev.*, D 33, 3487 (1986).
19. Stacey F. D. Gravity. *Science Progress*, vol. 69, No. 273, pp. 1–17, (1984).
20. Quinn T., Speake C. The Newtonian constant of gravitation – a constant too difficult to measure? An introduction. *Phil. Trans. Royal Society A* 372, 20140253.
21. Yanpeng Li. A Possible Exact Solution for the Newtonian Constant of Gravity. *British Journal of Mathematics and Computer Science*, vol. 19(3), 1–25, (2016).
22. Pound R. V., Rebka Jr. G. A. Gravitational Red-Shift in Nuclear Resonance. *Physical Review Letters*, 3 (9): 439–441, (1959).
23. Müller On the Acceleration of Free Fall inside Polyhedral Structures. *Progress in Physics*, 2018, vol. 14, 220–225.
24. Dermott S. F. On the origin of commensurabilities in the solar system - II: The orbital period relation. *Mon. Not. R. Astron. Soc.*, 141 (3): 363–376, (1968)
25. Lovis C. et al. The HARPS search for southern extra-solar planets. *Astronomy and Astrophysics*, manuscript Nr. HD10180, ESO, (2010)
26. Colombo G. Rotational Period of the Planet Mercury. *Letters to Nature*, Nr. 5010, p. 575, (1965)
27. Müller H. On the Cosmological Significance of Euler's Number. *Progress in Physics*, 2019, v. 15, 17–21.
28. Dombrowski K. Rational Numbers Distribution and Resonance. *Progress in Physics*, 2005, v. 1, no. 1, 65–67.
29. Müller H. The Physics of Transcendental Numbers. *Progress in Physics*, 2019, vol. 15, 148–155.
30. Müller H. Global Scaling. The Fundamentals of Interscalar Cosmology. *New Heritage Publishers*, Brooklyn, New York, USA, ISBN 978-0-9981894-0-6, (2018).
31. Müller H. Fractal Scaling Models of Natural Oscillations in Chain Systems and the Mass Distribution of Particles. *Progress in Physics*, 2010, v. 6, 61–66.
32. Müller H. Scale-Invariant Models of Natural Oscillations in Chain Systems and their Cosmological Significance. *Progress in Physics*, 2017, v. 13, 187–197.
33. Khintchine A.Ya. Continued fractions. University of Chicago Press, Chicago, (1964).
34. Hilbert D. Über die Transcendenz der Zahlen e und π . *Mathematische Annalen*, 43, 216–219, (1893).
35. Panchelyuga V.A., Panchelyuga M. S. Resonance and Fractals on the Real Numbers Set. *Progress in Physics*, 2012, v. 8, no. 4, 48–53.
36. Müller H. Quantum Gravity Aspects of Global Scaling and the Seismic Profile of the Earth. *Progress in Physics*, 2018, vol. 14, 41–45.
37. Müller H. Emergence of Particle Masses in Fractal Scaling Models of Matter. *Progress in Physics*, 2012, v. 8, 44–47.
38. Ries A. Bipolar Model of Oscillations in a Chain System for Elementary Particle Masses. *Progress in Physics*, 2012, vol. 4, 20–28.
39. Ries A. Qualitative Prediction of Isotope Abundances with the Bipolar Model of Oscillations in a Chain System. *Progress in Physics*, 2015, vol. 11, 183–186.
40. Ries A., Fook M. Fractal Structure of Nature's Preferred Masses: Application of the Model of Oscillations in a Chain System. *Progress in Physics*, 2010, vol. 4, 82–89.
41. Tanabashi M. et al. (Particle Data Group), *Phys. Rev. D* 98, 030001 (2018), www.pdg.lbl.gov
42. Astrophysical constants. Particle Data Group, pdg.lbl.gov
43. Planck M. Über Irreversible Strahlungsvorgänge. *Sitzungsbericht der Königlich Preußischen Akademie der Wissenschaften*, 1899, v.1, 479–480.
44. Müller H. Gravity as Attractor Effect of Stability Nodes in Chain Systems of Harmonic Quantum Oscillators. *Progress in Physics*, 2018, vol. 14, 19–23.
45. Müller H. Global Scaling of Planetary Atmospheres. *Progress in Physics*, 2018, v. 14, 66–70.
46. NASA Planetary Fact Sheet - Metric (2019).
47. Bills B. G., Ray R. D. Lunar Orbital Evolution: A Synthesis of Recent Results. *Geophysical Research Letters*, v. 26, Nr. 19, pp. 3045–3048, (1999).
48. Catalog of Exoplanets. Observatoire de Paris, <http://exoplanet.eu/catalog/>
49. Jacobson R. A. et al. The gravity field of the saturnian system from satellite observations and spacecraft tracking data. *The Astronomical Journal*, vol. 132, 2520–2526, (2006).
50. Jacobson R. A. The orbits of the uranian satellites and rings, the gravity field of the uranian system. *The Astronomical Journal*, vol. 148, 76–88, (2014).
51. Petropoulos A. E. Problem Description for the 6'h Global Trajectory Optimisation Competition. *Jet Propulsion Laboratory*, California Institute of Technology, (2012).